[73]D. Blechschmidt, M. Skibowski, and W. Steinmann, Opt. Commun. 1, 275 (1970).

[74]T. Sasaki, Y. Iguchi, H. Sugawara, S. Sato, T. Nasu, A. Ejiri, S. Onari, K. Kojima, and T. Oya, J. Phys. Soc. Japan 30, 580 (1971).

[75]H. Sugawara, T. Sasaki, Y. Iguchi, S. Sato, T. Nasu, A. Ejiri, S. Onari, K. Kojima, and T. Oya, Opt. Commun. 2, 333 (1970).

[76]R. Haensel, G. Keitel, G. Peters, P. Schreiber, B. Sonntag, and C. Kunz, Phys. Rev. Letters 23, 530 (1969).

[77]We assume here that the peaks are not simply a manifestation of structure in ϵ_2 (which might arise, e.g., from a dependence of the electron escape probability on the penetration depth of the light).

[78]J. C. Phillips, in *Solid State Physics*, edited by H. Ehrenreich, F. Seitz, and B. Turnbull (Academic, New York, 1966), Vol. 18, p. 131.

[79]U. Fano, Phys. Rev. 124, 1866 (1961).

[80]A classic example of this selection rule occurs in autoionization of the helium atom [see, e.g., E. U. Condon and G. H. Shortley, *The Theory of Atomic Spectra* (Cambridge U.P., New York, 1963), p. 371]. There, CI arises because of the Coulomb repulsion between the two electrons. This causes a discrete state of the atom to decay nonradiatively into a continuum state composed of a free electron and the He^+ ion. The process is described by the matrix element in (6) if the electron and hole states are replaced by the two electron states. The selection rule for the transition is then $\Delta J = \Delta P$ (parity) $= \Delta L = \Delta S = 0$.

[81]We assume that no other strong decay processes (besides direct radiative, Auger, and Coulombic CI decay) are present.

[82]F. C. Brown, C. Gähwiller, H. Fujita, A. B. Kunz, W. Scheifley, and N. Carrera, Phys. Rev. B 2, 2126 (1970).

[83]T. Sagawa, Y. Iguchi, M. Sasanuma, T. Nasu, S. Yamaguchi, S. Fujiwara, M. Nakamura, A. Ejiri, T. Masuoka, T. Sasaki, and T. Oshio, J. Phys. Soc. Japan 21, 2587 (1966).

[84]M. Cardona, R. Haensel, D. W. Lynch, and B. Sonntag, Phys. Rev. B 2, 1117 (1970).

[85]Y. Iguchi, T. Sagawa, S. Sato, M. Watanabe, H. Yamashita, A. Ejiri, M. Sasanuma, S. Nakai, M. Nakamura, S. Yamaguchi, Y. Nakai, and T. Oshio, Solid State Commun. 6, 575 (1968).

[86]S. Sato, T. Ishii, I. Nagakura, O. Aita, S. Nakai, M. Yokota, K. Ichikawa, G. Matsuoka, S. Kono, and T. Sagawa, J. Phys. Soc. Japan 20, 459 (1970).

[87]F. C. Brown, C. Gähwiller, A. B. Kunz, and N. O. Lipari, Phys. Rev. Letters 25, 927 (1970).

[88]N. O. Lipari and A. B. Kunz, Phys. Rev. B 3, 491 (1971).

[89]S. Nakai, T. Ishii, and T. Sagawa, J. Phys. Soc. Japan 30, 428 (1971).

[90]R. S. Bauer and W. E. Spicer, Phys. Rev. Letters 25, 1283 (1970).

[91]M. Cardona, *Modulation Spectroscopy*, Suppl. II of *Solid State Physics*, edited by C. B. Duke (Academic, New York, 1969), pp. 150 and 284.

[92] D. L. Camphausen, G. A. N. Connell, and W. Paul, Phys. Rev. Letters 26, 184 (1971).

PHYSICAL REVIEW B VOLUME 5, NUMBER 2 15 JANUARY 1972

A Self-Consistent Procedure for the Linear-Combination-of-Atomic-Orbitals Method: Application to LiF†

D. M. Drost* and J. L. Fry‡

Department of Physics and Astronomy, Louisiana State University, Baton Rouge, Louisiana 70803

(Received 23 August 1971)

An efficient method for computing self-consistent energy bands within the framework of the linear-combination-of-atomic-orbitals (LCAO) method is applied to LiF. Efficiency of the method is a result of characteristically small LCAO secular determinants, the ease with which energy bands may be computed at general points in the Brillouin zone, and a formalism which expresses iterated-Hamiltonian matrix elements in terms of LCAO integrals computed in the first step only. A study of the self-consistent procedure is presented, including an investigation of convergence and accuracy. On the basis of this study it is concluded that self-consistent calculations using small Brillouin-zone samplings of symmetry points to compute charge densities contain errors as large as 1 eV. Accurate self-consistent energy bands are computed for LiF in the Hartree-Fock-Slater approximation and compared with previous calculations and experimental data. While an initial linear combination of ionic potentials with an adjustable exchange potential yields reasonable agreement with optical data, only a self-consistent potential produces agreement with both optical and photoemission data. It is suggested that to obtain reliable spectra, even when using an adjusted exchange potential, it is necessary to compute optical properties with self-consistent energy bands and wave functions.

I. INTRODUCTION

In the last five years there has been renewed interest in the linear-combination-of-atomic-orbitals (LCAO) method for obtaining energy bands in solids. Although it is the oldest method of band calculation,[1] poor results from early inappropriate approximations caused it to fall into disfavor for a few decades.

The advent of modern high-speed computers, new mathematical techniques, and increasing interest in transition metals and their compounds led to a reexamination of the LCAO method, both in first principles[2,3] and pseudopotentials[4] or interpolation[5] applications. While other methods[6] of band calculation exist which yield accurate band energies at symmetry points in the Brillouin zone for certain model potentials, the LCAO method places fewer limitations on the type of crystalline potential and has the advantage that it can easily produce band energies at arbitrary points in the zone. The LCAO method usually results in a relatively small secular determinant, but only at the expense of matrix elements which are more costly to compute. Adoption of Gaussian-type atomic orbitals and techniques of accelerating convergence of sums[7,8] have made the LCAO method competitive in speed with other standard techniques.

In a previous report[9] Callaway and Fry outlined a procedure for computing self-consistent energy bands within the framework of the LCAO method (referred to in this paper as the SCLCAO method). In essence it is a method of obtaining SCLCAO energy bands without computing new LCAO integrals at each iteration. This technique for generating self-consistent energy bands is tested here by applying it to the simplest alkali-halide, LiF, and it is found to be quite efficient.

While energy-band theory has progressed during the last decade, it has not yet reached a state of development comparable to the self-consistent field theory of atomic structure. There have been only a few attempts to make truly self-consistent energy-band calculations from first principles. The major efforts in this direction have been with the orthogonalized-plane-wave (OPW) method,[10,11] the local orbital method[12] and the augmented-plane-wave method (APW).[13,14]

In the APW method a muffin-tin potential is usually employed, so that charge within the atomic sphere and charge without are treated differently in the self-consistent scheme. During iterative cycles charge moves in and out of the sphere, and it may not be possible to arrive at a stable self-consistent result. Even when it is possible, the results obtained would have to be described as self-consistent within the muffin-tin constraint. While methods of improving the muffin-tin approximation exist,[14] a self-consistent APW calculation using the methods is a very ambitious project at present.

The OPW method also makes an artificial division between core and valence states. It requires that a self-consistent cycle consist of two steps, one for core and one for valence. But this is merely an inconvenience and presumably places little or no constraint upon the final self-consistent charge distribution in the crystal. By adding the core states to the basis of plane waves instead of orthogonalizing to them, the self-consistent calculation would procede more naturally and easily. In this case, as with the mixed basis used in local-orbital calculations, the method described in this paper could be used to obtain self-consistency.

The purpose of this paper is to study the SCLCAO procedure and examine effects of self-consistency upon the energy bands and wave functions in LiF. Some conclusions reached here are unexpected, but are believed to hold for other crystals as well. The remainder of this paper is organized as follows. In Sec. II a brief outline of the SCLCAO procedure is presented. Section III describes the initial LCAO band structure for LiF, and Sec. IV details the self-consistent calculations. Section V makes contact with experiment and compares initial and final energy bands. Section VI contains concluding remarks.

II. SELF-CONSISTENT PROCEDURE

In this section the essential equations for the SCLCAO method are presented.[9] The fundamental problem in a self-consistent calculation is to determine a new potential after a given stage of band-structure calculation has been completed. The energy bands $E_n(\vec{k})$ and Bloch functions $\Psi_n(\vec{k},\vec{r})$ are obtained from a starting potential and a variational basis set by simultaneous diagonalization of Hamiltonian and overlap matrices. The Bloch solutions are expressed as

$$\Psi_n(\vec{k},\vec{r})=\sum_i a_{ni}(\vec{k})\psi_i(\vec{k},\vec{r}), \tag{1}$$

where the coefficients a_{ni} are determined by the diagonalization process and $\psi_i(\vec{k},\vec{r})$ are linear combinations of atomic (or individual) orbitals u_i localized on sites $\vec{R}_\mu$:

$$\psi_i(\vec{k},\vec{r})=(1/N^{1/2})\sum e^{i\vec{k}\cdot\vec{R}_\mu}\,u_i(\vec{r}-\vec{R}_\mu). \tag{2}$$

The summation is over all N lattice sites $\vec{R}_\mu$, and the coefficients $e^{i\vec{k}\cdot\vec{R}_\mu}$ ensure that the basis functions $\psi_i(\vec{k},\vec{r})$ satisfy Bloch's theorem. For simplicity, the equations in this section are written for a monatomic lattice. Generalization to polyatomic crystals is straightforward.

A. Iterated Coulomb Potential

The iterated potential is computed from the crystal charge density corresponding to the solutions given by Eq. (1). In the LCAO method employed here it is the Fourier transform of the crystal potential which is required. This may be obtained from the charge density using Poisson's equation

$$V(\vec{K})=-8\pi\rho_T(\vec{K})/K^2, \tag{3}$$

in atomic units with energy measured in rydbergs. $\rho_T(\vec{K})$ is the Fourier coefficient of the total charge

density. The Fourier coefficients of the electron charge density are given by

$$\rho(\vec{K}) = (1/N\Omega) \int \rho(\vec{r})\, e^{-\vec{K}\cdot\vec{r}} d^3r \ , \tag{4}$$

with Ω the unit cell volume, N the number of unit cells in the crystal, and

$$\rho(\vec{r}) = \sum_{n,\vec{k},\mathrm{occ}} |\psi_n(\vec{k},\vec{r})|^2 \ . \tag{5}$$

Substituting (1), (2), and (5) into (4) and converting the sum on $\vec{k}$ to an integral one obtains

$$\rho(\vec{K}) = \frac{1}{(2\pi)^3} \sum_{n,i,j} \int d^3k\, a^*_{ni}(\vec{k}) S_{ij}(\vec{k},\vec{K}) a_{nj}(\vec{k}) \ , \tag{6}$$

where the integral is over the portion of the Brillouin zone in which band n is occupied. S_{ij} is a generalized overlap matrix defined by

$$S_{ij}(\vec{k},\vec{K}) = \sum_\sigma e^{i\vec{k}\cdot\vec{R}_\sigma} \int u^*_i(\vec{r})\, e^{-i\vec{K}\cdot\vec{r}}\, u_j(\vec{r}-\vec{R}_\sigma) d^3r \ . \tag{7}$$

For $K = 0$, Eq. (3) fails and a limiting procedure must be used:

$$V(0) = -8\pi \lim [\rho_T(K)/K^2] \ \text{ as } \vec{K} \to 0. \tag{8}$$

The limit exists and may be expressed as

$$V(0) = \frac{1}{6\pi^2} \sum_{nij} \int a^*_{ni}(\vec{k}) S^{(2)}_{ij} \rho(\vec{k}) a_{nj}(\vec{k}) d^3k \ , \tag{9}$$

where the integral again is over the occupied part, and

$$S^{(2)}_{ij}(\vec{k}) = \sum_\sigma e^{i\vec{k}\cdot\vec{R}_\sigma} \int u^*_i(\vec{r}) r^2 u_j(\vec{r}-\vec{R}_\sigma) d^3r \ . \tag{10}$$

The utility of these expressions is obvious when it is realized that the quantity S_{ij} is related to the Hamiltonian matrix elements

$$\begin{aligned} &\int \psi^*_i(\vec{k},\vec{r})\, V(\vec{r}) \psi_j(\vec{k},\vec{r}) d^3r \\ &\quad = \sum_{s,\sigma} V(\vec{K}_s) e^{i\vec{k}\cdot\vec{R}_\sigma} \int u^*_i(\vec{r})\, e^{i\vec{K}_s\cdot\vec{r}}\, u_j(\vec{r}-\vec{R}_\sigma) d^3r \\ &\quad = \sum_s V(\vec{K}_s) S_{ij}(\vec{k}, -\vec{K}_s) \ , \end{aligned} \tag{11}$$

where $V(\vec{r})$ is the periodic crystal potential. For a fixed set of basis functions and a given lattice constant, the integrals appearing in (10) and (11) need be computed only once and saved. In subsequent iterations the only quantities which change in the Hamiltonian matrix as expressed in Eq. (11) are the Fourier coefficients of the potential, which are given by Eqs. (3), (6), and (9). Thus, an iterative cycle is established which requires none of the lengthy integral computations encountered in the initial band calculation. Since the last expression for the Hamiltonian matrix elements in Eq. (11) may be evaluated very rapidly, the time required for a complete iteration is just the time needed to diagonalize the Hamiltonian and overlap matrices at the grid points selected in the Brillouin zone for doing the integrals in Eq. (6).

The chief limitation in applying these equations efficiently is data handling. The size of the four-dimensional array $S_{ij}(\vec{k}, \vec{K}_s)$ may get very large, depending upon the sampling in $\vec{k}$ required and upon the number of reciprocal-lattice vectors $\vec{K}_s$ needed. These details are discussed in Sec. III.

B. Iterated Exchange Potential

It is assumed that a local-exchange approximation is made in the band calculation, for example, the "$X\alpha$" approach,[15] with an exchange potential proportional to $\rho^{1/3}(\vec{r})$. In the initial band calculation it is necessary to compute the Fourier transform of $\rho^{1/3}(\vec{r})$, but in subsequent iterations it is more convenient to Fourier-transform the difference between $\rho^{1/3}(\vec{r})$ and $\rho_0^{1/3}(\vec{r})$:

$$\Delta(\vec{r}) = \rho^{1/3}(\vec{r}) - \rho_0^{1/3}(\vec{r}) = \sum_s \Delta(\vec{K}_s)\, e^{i\vec{K}_s\cdot\vec{r}} \ . \tag{12}$$

By expanding $\rho(\vec{r})$ and $\rho_0(\vec{r})$ in a Fourier series and extracting the cube root, it is possible to determine $\Delta(\vec{K})$:

$$\begin{aligned} \Delta(\vec{K}) = \tfrac{1}{3}\left(\frac{\Omega}{n_e}\right)^{2/3} \Big[&\rho(\vec{K}) - \rho_0(\vec{K}) \\ &- \tfrac{2}{3}\left(\frac{\Omega}{n_e}\right) \sum_{t\neq 0} [\rho(\vec{K}_t)\, \rho(\vec{K}-\vec{K}_t) \\ &- \rho_0(\vec{K}_t)\rho_0(\vec{K}-\vec{K}_t)] + \cdots \Big], \end{aligned} \tag{13}$$

where n_e is the number of electrons in a unit cell. For $\vec{K} = 0$, one has

$$\begin{aligned} \Delta(0) = -\tfrac{2}{9}\, (\Omega/n_e)^{5/3} \sum_t [&\rho(\vec{K}_t)\, \rho(-\vec{K}_t) \\ &- \rho_0(\vec{K}_t)\, \rho_0(-\vec{K}_t)] \ , \end{aligned}$$

to second order.

III. APPLICATION TO LiF

LiF was picked as a simple example to test the SCLCAO method of Sec. II. It is simple in two respects. First, it is composed of two light elements with only a few electrons each, so that the LCAO secular determinant is small. For purposes of computing charge densities and iterated potentials, no d wave functions are important. The second major simplification occurs because LiF is an insulator: There is no need to compute the Fermi energy for each iteration to determine occupied and empty levels. Generation of self-consistent potentials is a considerably more sensitive process for metals, especially when a small sampling of states in the Brillouin zone is used.

TABLE I. Gaussian wave functions.

α_s	c_{1s}	c_{2s}	α_p	c_{2p}
		Lithium		
3 184.4671	0.000 29	−0.000 05	0.022 943 4	0.006 285
480.512 66	0.002 24	−0.000 35	0.076 491 8	0.032 22
108.863 25	0.011 73	−0.001 84	0.444 620	0.063 23
30.289 479	0.048 10	−0.007 66	1.156 85	−0.027 82
9.641 513 7	0.148 52	−0.024 42	3.157 89	0.107 31
3.391 555 9	0.320 38	−0.057 25	9.353 29	−0.063 58
1.272 028 5	0.421 13	−0.098 17	31.941 5	0.118 99
0.496 432 05	0.204 75	−0.123 82		
0.097 186 33	0.009 22	0.252 85		
0.049 988 14	−0.004 58	0.545 20		
0.022 952 09	0.001 39	0.305 37		
		Fluorine		
37 736.000	0.000 22	−0.000 05	102.40	0.004 29
5 867.079 1	0.001 63	−0.000 38	23.794 387	0.030 81
1 332.467 9	0.008 68	−0.002 04	7.495 459 0	0.118 92
369.858 66	0.036 43	−0.008 50	2.763 871 3	0.269 64
117.129 69	0.122 88	−0.030 75	1.099 057 5	0.362 25
40.302 862	0.309 44	−0.083 18	0.451 354 09	0.330 00
14.898 010	0.440 64	−0.170 29	0.172 139 36	0.153 23
5.877 735 9	0.221 46	−0.108 32		
1.626 760 6	0.014 55	0.379 80		
0.610 724	−0.002 30	0.568 88		
0.233 411 5	0.000 92	0.201 56		

A. Initial Band Structure

The initial band structure was computed using methods previously described.[3] The Coulomb potential was constructed as a superposition of atomic potentials, while the exchange potential was approximated by $\rho^{1/3}(\vec{r})$, where $\rho(\vec{r})$ is the crystalline charge density computed in the first iteration as a linear superposition of the ionic charge densities. In the first attempt to obtain LiF energy bands, atomic wave functions u_i of Eq. (2) consisted of linear combinations of Slater-type[16] orbitals (STO), but, subsequently, Gaussian-type[17] orbitals (GTO) were used to reduce computer times. Atomic orbitals used included $1s$, $2s$, and $2p$ for lithium and $1s$, $2s$, and $2p$ for fluorine. The GTO wave functions used are shown in Table I and energy bands obtained with them from the starting potential are shown in Fig. 1.

Only the highest valence (mainly fluorine $2p$) and lowest conduction band (lithium $2s/2p$) are shown at this stage of the calculation. Three sets of bands are shown corresponding to different "$X\alpha$" exchange potentials: Slater, $\alpha=1$; Kohn-Sham-Gaspar, $\alpha=\frac{2}{3}$; and a fit to experimental gap, $\alpha=\frac{3}{4}$. This latter value differs from the value required to fit the fundamental gap in a previously reported APW calculation[18] of the energy bands of LiF ($\alpha=1$). This disagreement may reflect differences in crystal potentials (the APW calculation used a point-charge approximation when calculating non-spherical terms), or lack of convergence in one of the band calculations. The former is probably the proper explanation since exhaustive studies of convergence have been made in this effort, and convergence properties of the APW method are well understood.

Nothing remarkable appears in Fig. 1. The minimum gap appears at Γ, where the lowest conduction band is s like. At X and L it is p like. Reduction of the strength of the exchange potential raises and slightly broadens the energy bands with no dramatic structural changes occurring, since no complicated hybridization of bands is present.

In SCLCAO calculations there are five types of "convergence" which must be obtained: (i) Convergence of the Fourier series in Eq. (11) (sum over reciprocal-lattice vectors), (ii) convergence of the Bloch sum in Eq. (11) (sum over firect-lattice neighbors), (iii) convergence of the sum in Eq. (1) with respect to addition of more basis functions, (iv) "convergence" of the Brillouin-zone integration scheme for Eq. (6) with respect to finer sampling methods, and (v) convergence of the iterative cycles to a self-consistent result.

Each type of convergence is crucial to accuracy in the final energy bands, so examples of each are given in this paper for future guidelines. The first three types are discussed here, and the last two are considered in Secs. III C and III D.

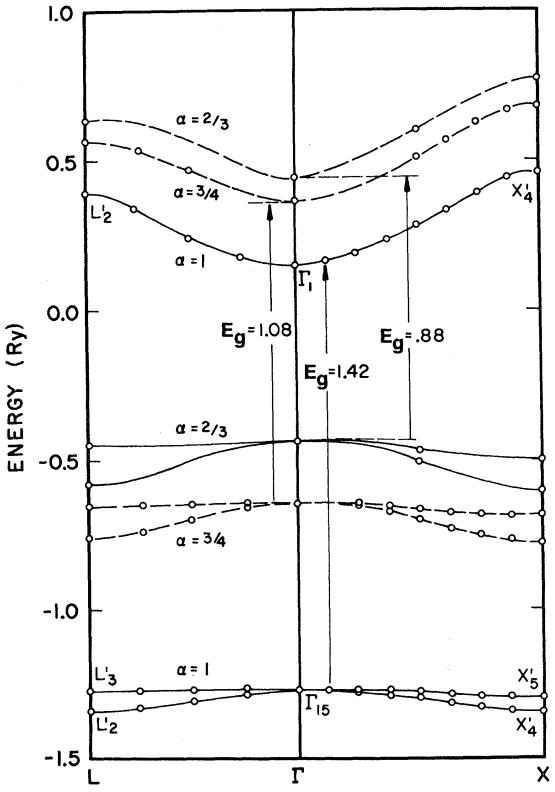

FIG. 1. LiF Bands from atomic superposition. The lattice constant used throughout this paper is 4.0173 Å.

1. *Reciprocal-Lattice Convergence*

The original STO band structure was abandoned because it was too time consuming to obtain adequate convergence of reciprocal-lattice sums. STO bands obtained at different stages of convergence of the Fourier series are shown in Fig. 2. As the number of reciprocal-lattice vectors (RLV) used to compute s-s- and s-p-type integrals was increased, the Γ_1 conduction band slowly converged toward the Γ_{15} conduction band, and the spurious oscillations along the Δ axis smoothed out. The dashed curve was obtained with a typical s-p integral summed to 38 independent magnitudes (or stars) of RLV, while the solid curve was obtained from s-p integrals summed to 800 independent magnitudes of RLV. Inadequate convergence was still reflected in the incorrect ordering of the Γ_1 and Γ_{15} levels.

Direct summation of the Fourier series of Eq. (11) to convergence was not found to be practical using STO basis functions because complexity of integral expressions and slowness of the numerical integration required very excessive computer costs. Techniques for handling this type of convergence difficulty are available,[7] but it was decided to convert the basis set to GTO before using them. Computations were then made much easier because analytic expressions exist for all integrals, and computer times were greatly reduced. Table II shows representative integrals and their convergence properties. The GTO integrals were converged until summing a substantial number of additional RLV caused changes of less than 0.001 Ry in any energy bands. A comparison at the midpoint of the Δ axis in the Brillouin zone is made in Table III between unconverged STO matrix elements and converged GTO matrix elements. Differences are typically small, but enough to reorder the s and p bands at Γ and remove spurious oscillations of the p bands.

As a rule, valence bands were much less sensitive to problems of convergence, either direct or reciprocal lattice, then the conduction bands. The self-consistent valence bands and potentials reported below would not be influenced by more stringent convergence criteria. Conduction bands are believed converged to less than 0.01 Ry with respect to both reciprocal- and direct-lattice sums.

2. *Direct-Lattice Convergence*

The number of neighbors required for direct-lattice convergence depends upon the type of integral computed. Insufficient convergence was always reflected by negative overlap eigenvalues for conduction bands. The number of neighbors used for different integrals is shown in Table IV.

TABLE II. Convergence of reciprocal-lattice sums for various integrals (energy in Ry).

No. of stars	$L(2s)F(2p_z)$	$F(2p_x)F(2p_y)$	$F(2s)F(2p_x)$	$L(2s)L(2p_x)$	$F(2s)L(2p_z)$
423	−1.460 778	0.011 771	−0.017 384	−0.222 361	−0.034 388
810	−1.480 798	0.011 768	−0.017 433	−0.222 439	−0.034 405
1185	−1.489 131	0.011 768	−0.017 450	−0.222 448	−0.034 408
3000	−1.498 195				
		$L(2s)L(2s)$			$L(2s)F(2s)$
10 000		−0.283 141			−0.271 089
15 000		−0.283 139			−0.270 933
20 000		−0.283 137			−0.270 857

TABLE III. Comparison of unconverged STO matrix elements and converged GTO matrix elements (energy in Ry).

Matrix element	STO	GTO
$L(2s)L(2s)$	−1.7677	−1.7663
$L(2p_x)L(2p_x)$	−7.7457	−7.8132
$L(2s)L(2p_x)$	−3.5671	−3.5750
$F(2p_x)F(2p_x)$	−1.5158	−1.3483
$L(2s)F(2p_x)$	−0.9390	−0.6519
$L(2p_x)F(2p_x)$	−1.9830	−1.3310

It is interesting to think of the LCAO calculation as a giant molecular-orbital (MO) calculation. From that point of view the minimum number of atoms required to make a LiF crystal, as far as the lowest conduction bands are concerned, is about 4500. By then all of the properties of the crystal necessary to produce energy bands satisfying Bloch's theorem will have been realized by at least one electron near the central atom. As more atoms are added, more electrons near the center will see a "periodic" potential. The number of bandlike electrons would rapidly increase. When bandlike electrons greatly outnumber "surface" electrons, bulk electronic properties would presumably be perfect-crystal-like. Assuming a spherical distribution, this would occur for $\Delta N/N \ll 1$, where ΔN is the number of atoms in the surface region and N is the number of atoms in the body of the crystal about the central atom. Thus, bulk properties of LiF depending upon detailed structure of the lowest conduction band would be exhibited by a large molecule with 225 nearest-neighbor sets, corresponding to $\Delta N/N \approx 0.1$. In terms of a thin film, this is a thickness of 904 Å.

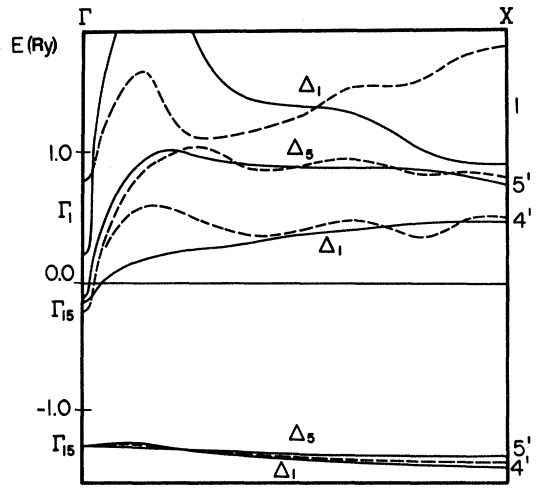

FIG. 2. Unconverged STO bands of LiF. The solid curves contained more terms in the reciprocal lattice, but are not completely converged.

3. *Convergence of Basis Set*

The basis set used for the LCAO calculation may be improved in two ways: First, nonlinear variations in the individual orbitals could be permitted, i.e., variation of the parameter in the orbital exponent. For a reasonable set of starting functions in atomic calculations these variations produce changes which are smaller than other errors in this calculation. On the other hand, the addition of more basis functions can affect the energy bands substantially.

By varying the size of the basis set in this and previous calculations it has been found that lower-lying bands are insensitive to additional functions, but the highest band of each symmetry type can be readily influenced. It has usually been sufficient to include one more band of a given symmetry, represented by a well-chosen function, to obtain convergence to less than 0.1 eV for the last band of that same symmetry. This will vary from crystal to crystal depending upon choice of basis functions and the number of bands of the same symmetry lying close in energy to the one under consideration.

Because of the difficulty in computing LCAO matrix elements, the total number of basis functions or energy bands to be retained must be decided with care. In this calculation all bands through the lowest conduction band are believed to be converged to better than 0.1 eV with respect to the basis set.

IV. SELF-CONSISTENT LiF ENERGY BANDS

With properly converged first-iteration energy bands it was possible to proceed to the self-consistent calculation and study the behavior of the equations of Sec. II with reasonable assurance that any peculiarities were due to the procedures and not to errors in the initial energy bands and wave functions.

A. Computation of $S_{ij}(\vec{k}, \vec{K}_n)$

The fundamental quantity which is needed for the SCLCAO equations is the generalized overlap matrix $S_{ij}(\vec{k}, \vec{K}_n)$ of Eq. (7). This quantity must be computed and stored for reuse at successive iterations. Computation of S_{ij} is straightforward: It

TABLE IV. Number of direct-lattice neighbors used for different integrals.

Integral	Neighbors	Integral	Neighbors
$L(s)L(s)$	75	$F(s)F(p)$	5
$L(p)L(p)$	75	$L(s)F(s)$	30
$L(s)L(p)$	75	$L(p)F(p)$	50
$F(s)F(s)$	3	$L(s)F(p)$	30
$F(p)F(p)$	10	$F(s)L(p)$	30

TABLE V. *Self-consistent corrections to Fourier coefficients of Coulomb potential.* AS means atomic superposition, SC means self-consistent. The prime indicates equal-volume weights used; unprimed grid numbers refer to nearest-volume weights (units are Ry).

$\vec{K}_n$	(000)	(111)	(200)	···	(731)
V(nuclear)	···	0.670 86	−1.006 28	···	0.034 11
V_e (AS)	−0.675 39	0.089 65	−0.271 42	···	0.000 37
ΔV_e(4, SC)	−0.183 7	0.003 67	−0.002 02	···	0.000 06
ΔV_e(6, SC)	0.101 95	0.003 46	−0.001 65	···	0.000 02
ΔV_e(6′, SC)	0.164	−0.029 8	0.023 44	···	0.000 02
ΔV_e(20′, SC)	0.215 8	0.007 87	−0.004 46	···	0.000 00
ΔV_e(89′, SC)	0.190 9	0.009	−0.005	···	0.000 00
ΔV_e(89′, 1st)	0.199 37	0.005 32	−0.003 14	···	0.000 06

has exactly the same form as an LCAO Hamiltonian or overlap matrix. In fact, the same computer programs may be used, although it is better to revise them to avoid repeated calculation of identical quantities for each $\vec{K}_n$. The size of the array $S_{ij}(\vec{k}, \vec{K}_n)$ depends upon the number of points $\vec{k}$ in the Brillouin zone needed to perform the integral of Eq. (6) and also the number of RLV necessary to describe changes in the crystal potential from one iteration to the next. While several different $S_{ij}(\vec{k}, \vec{K}_n)$ array sizes were tested for LiF, it was found that a $10\times10\times89\times25$ array gave best results in terms of accuracy achieved for reasonable computer core requirements and time used. This S_{ij} was a 10×10 matrix computed for 89 points in $\frac{1}{48}$ of the fcc Brillouin zone for only 25 different magnitudes of $\vec{K}_n$.

The generalized overlap matrix $S_{ij}(\vec{k}, \vec{K}_n)$ does not transform like $\rho(\vec{K}_n)$, i.e., the Γ_1 irreducible representation, yet it is necessary to compute S_{ij} only for points within $\frac{1}{48}$ of the Brillouin zone if the sums on indices i and j are also performed, as in computing $\rho(\vec{K})$ via Eq. (6). Computation of $S_{ij}(\vec{k}, \vec{K}_n)$ for a given sampling of points $\vec{k}$ is equivalent to computing the Hamiltonian matrix over the same grid, and it must be done for all $\vec{K}_n$ which contribute to changes in the band structure via $\rho(\vec{K}_n)$, so not only can the size of the array get too large and cause data handling problems, but the time required to compute S_{ij} may become substantial, depending upon how many direct-lattice vectors (DLV) must be summed in Eq. (7). It is important to keep indices $\vec{k}$ and $\vec{K}_n$ as small as possible.

B. Iterated Potential Coefficients

Clearly, the usefulness of Eq. (6) is limited to changes in potential from one iteration to the next which can be described by a few Fourier coefficients. In addition, Eq. (13) is useful only if the changes are small enough that higher terms in the series are negligible. Both of these conditions will be met if the starting potential is well chosen and almost self-consistent. This will be easy for most simple insulators, but may be more difficult for transition metals. For LiF the superposition of ionic potentials was a good starting point. Table V shows the various contributions to the Fourier coefficients of the potentials and the changes which occur when the potential is made self-consistent. For large $\vec{K}_n$ the nuclear contributions (which remain fixed during all iterations) dominate. In addition, changes in the electronic Coulomb potential are caused primarily by rearrangement of valence charges, so that important changes in Fourier coefficients occur only for low $\vec{K}_n$. While some computations were performed retaining changes in the first 100 independent magnitudes of RLV, only 25 were retained in most of the results quoted below. This was more than adequate for the accuracy desired; usually half that number would have been enough. The accuracy of expression (13) for the exchange potential was good at first order in $\rho(\vec{K}_n)$, so second-order terms were neglected in order to avoid the fairly time consuming task of summing the Fourier product series for each value of $\vec{K}_n$.

C. Convergence of Iterative Cycles

There was no assurance that the iterative cycle established in Sec. II would stabilize to a self-consistent result. The first attempts at self-consistency were made using six points in $\frac{1}{48}$ of the zone, retaining 100 distinct magnitudes of $\vec{K}_n$ up to RLV (731). Computations proceed very rapidly because of the small secular determinant and the speed of Eq. (11) using $S_{ij}(\vec{k}, \vec{K}_n)$ to compute matrix elements.

For the six-point integration grid, changes computed in potential coefficients were always too drastic to lead to self-consistency rapidly, the result being that oscillations in the coefficients occurred from iteration to iteration. By taking a suitable average of the coefficients for the ith and $(i+1)$th iterations, the procedure was made to converge

TABLE VI. *Self-consistent iterations.* Changes in the valence-band maximum Γ_{15}, changes in the energy gap E_g and changes in Coulomb Fourier coefficients as they approach self-consistency are shown. $\alpha = 1$ exchange parameter, and $x = 0.25$ convergence factor were used with an 89-point integration grid (energy in Ry).

Iteration	Γ_{15}	E_g	$\Delta V(111)$	$\Delta V(200)$	$\Delta V(731)$
0	−1.2657	1.4224	0.002 66	−0.001 57	0.000 00
1	−1.0924	1.4504	0.004 50	−0.002 64	0.000 01
2	−1.1123	1.4689	0.005 77	−0.003 39	0.000 01
3	−1.1252	1.4812	0.006 67	−0.003 90	0.000 01
4	−1.1336	1.4895	0.007 30	−0.004 27	0.000 01
5	−1.1392	1.4952	0.007 75	−0.004 53	0.000 01
6	−1.1429	1.4990	0.008 07	−0.004 71	0.000 01
7	−1.1454	1.5017	0.008 30	−0.004 85	0.000 01

much more rapidly. Without a convergence factor, ten iterations were needed to stabilize energy bands to 0.001 Ry, but a crudely chosen convergence factor obtained the same results with only three iterations. The scheme used here was

$$V_{i+1}(\vec{K}_n) = xV_{i-1}(\vec{K}_n) + (1-x)V_i(\vec{K}_n),$$

where $0 \leq x < 1$ is the convergence factor, (which, in general, could be chosen different for different $\vec{K}_n$) and $V_{i-1}(\vec{K}_n)$ are the Fourier coefficients which gave energy bands and wave functions which, in turn, yielded new Fourier coefficients $V_i(\vec{K}_n)$. Successive iterations started with modified Fourier coefficients $V_{i+1}(\vec{K})$ instead of the directly computed $V_i(\vec{K})$. For small Brillouin-zone integration grids, small values of x gave better results ($x \approx 0.25$), while the 89-point grid worked better with larger values of x ($x \approx 0.75$). An example of an overcorrection using the 89-point grid and $x = 0.25$ is shown in Table VI. No oscillations are present, corrections at each iteration being in the same direction, but the rate of convergence is too slow. With $x = 0.75$ a similar accuracy was achieved in only three steps. For $x = 1$ oscillations occurred, but not as strong as with the six-point integrations grid.

Convergence properties of Coulomb-potential coefficients, fluorine $2p$ valence band, Γ_{15}, and the fundamental energy gap E_g shown in Table VI are typical of all calculations performed here. Corrections to the atomic superposition potential coefficients for RLV numbers 2, 3, and 25 are shown. The last contributes nothing: No changes would have occurred had only 10 RLV been retained instead of 25. During iterative cycles the higher coefficients always reached self-consistency first, so it was possible to monitor the first one or two during calculations to check over-all convergence rates. Convergence of the energy eigenvalues followed a similar pattern. Core levels became self-consistent rapidly, with valence next and then conduction levels.

D. Choice of Brillouin-Zone Grid

In order to perform a self-consistent energy-band calculation it is necessary to evaluate either the charge density or its Fourier transform by intergration over the occupied part of the Brillouin zone. Because of the difficulty of computing energy bands and wave functions at a large number of points k in the zone, this integration has always been replaced by a weighted sum over a very few points, usually symmetry points.[10,11] Symmetry points are not good representatives of the totality of points in the zone, and doubts about performing volume integrals with only six points were checked in this calculation, since a good sampling throughout the zone could be generated without difficulty. Suspicions were confirmed: Small samplings led to errors of the order of electron volts, which is substantially larger than previous estimates,[11] and one order of magnitude or so larger than experimental uncertainties.

The first self-consistent band structure for LiF was done with a six-point grid in the irreducible portion of the zone including the points Γ, Δ, X, Σ, W, and L, where Δ and Σ were chosen at the midpoints of the Δ and Σ axis. The computation was then repeated using 89 uniformly spaced points, with unexpected results. Figure 3 compares first-iteration bands (atomic superposition) with self-consistent six- and 89-point energy bands. The six-point formula raised the valence band by 0.5 Ry, reducing the fundamental gap from 1.42 to 0.928 Ry. On the other hand, the 89-point grid produced smaller changes, raising the bands slightly, but *increasing* the energy gap from 1.42 to 1.50 Ry. An additional check was made by running a 20-point grid of uniformly spaced points: The bands agreed to within 0.01 Ry with the 89-point results. These bands were too close to the 89-point bands to display clearly on the scale of the graph in Fig. 3 and are not shown. It must therefore be concluded that the six-point sampling yields a poor approximation to the true crystal charge

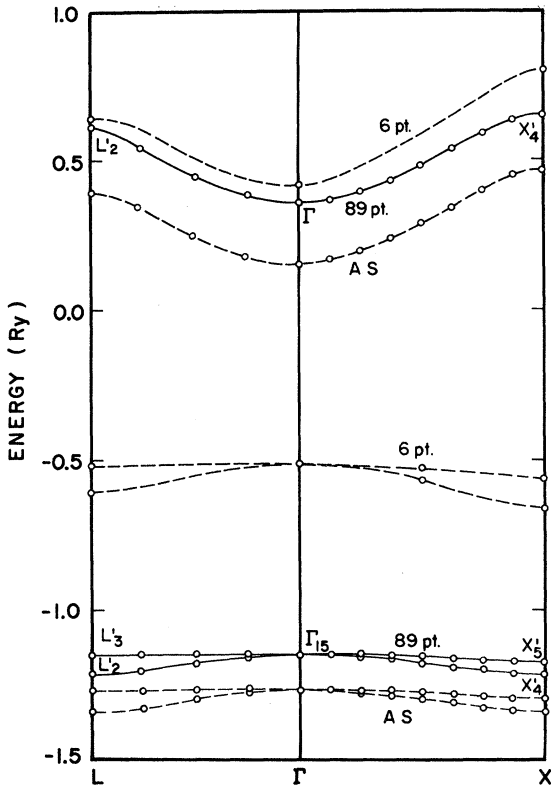

FIG. 3. Self-consistent LiF bands. These three sets of bands were computed using an $X\alpha$ exchange potential with $\alpha = 1$. AS means atomic superposition, non-self-consistent.

density. The 20- and 89-point grids produce charge densities much closer to the atomic superposition and yield energy bands not radically different from the initial band structure: A superposition of ionic potentials is a fairly good approximation to the self-consistent potential for LiF.

The last fact may be appreciated by examining Table V, which compares Fourier coefficients of the Coulomb potential. The first row is the nuclear contribution and the second row is the electronic contribution computed from the atomic superposition. Self-consistent corrections to be added to the second row for the six-, 20-, and 89-point grids are shown in the last four rows. While corrections to the electronic Coulomb coefficients are small in all cases, the six-point formula yields corrections which disagree both in sign and magnitude with the others. The last row of Table V shows ΔV_e computed from the initial band wave functions. Corrections computed at the first iteration and last iteration are rather close for the 89-point grid. X-ray form factors computed from the initial band structure would agree well with the self-consistent form factors, although errors larger than those associated with experimental measurements would still persist in the non-self-consistent result. This is not the case for the six-point grid: The initial potential is considerably more nearly self-consistent than the small grid would suggest, either after one iteration or after the last six-point iteration.

Since the six-point grid, contrary to previous reports, [11] yielded such poor results for LiF, further tests of the integration grid were made. In the grids discussed so far the integration weight factors associated with each grid point were computed in a standard way: Each point of the uniform grid was assumed to occupy the same volume of k space, weights differing from point to point only because parts of the volume for some points fell outside of the irreducible portion of the zone. This is referred to as the "equal-volume" set of weights.

Perhaps a more reasonable assignment of weights, especially for a small nonuniform grid, is the "nearest-volume" assignment, in which the weight assigned to a point is proportional to the volume of the zone which is closer to it than any other grid point in the zone. For a large number of points the two weighting schemes should yield very nearly identical results since symmetry points contribute little; i.e., they occupy a negligible volume of the zone.

The accuracy of the nearest-volume weights was checked by self-consistent calculations with the four- and six-point grids using weights given in Ref. 11. Energy bands are shown in Fig. 4 compared with the previous 89-point grid, and self-consistent corrections to the potential are shown in rows three and four of Table V (unprimed grid numbers). Comparison of energy gaps obtained from the nearest-volume grids and from the equal-volume grids at each stage of self-consistency is made in Table VII.

The following conclusions must be drawn. Energy bands for the four- and six-point nearest-volume-weight grids are different in absolute energy, mainly because of different signs on $V(000)$ shown in Table V, but energy differences computed from either set of bands would agree to within a few mRy, e.g., the fundamental gap shown in Table VII. This corresponds to the sort of "accuracy" estimated in Refs. 10 and 11. The surprising result is that these energy differences do not agree with the more accurate 20- and 89-point grids. Although the four- and six-point nearest-volume grids are in good agreement with each other and are better than the equal-volume 6-point grid, they are accurate to only 0.1 Ry when compared with the 89-point grid. The very close agreement between valence bands for the nearest-volume 6-point grid and the 89-point grid must be regarded as accidental. If $V(000)$ had been computed correctly with the six-point grid there would have been a constant shift upward of 0.1 Ry.

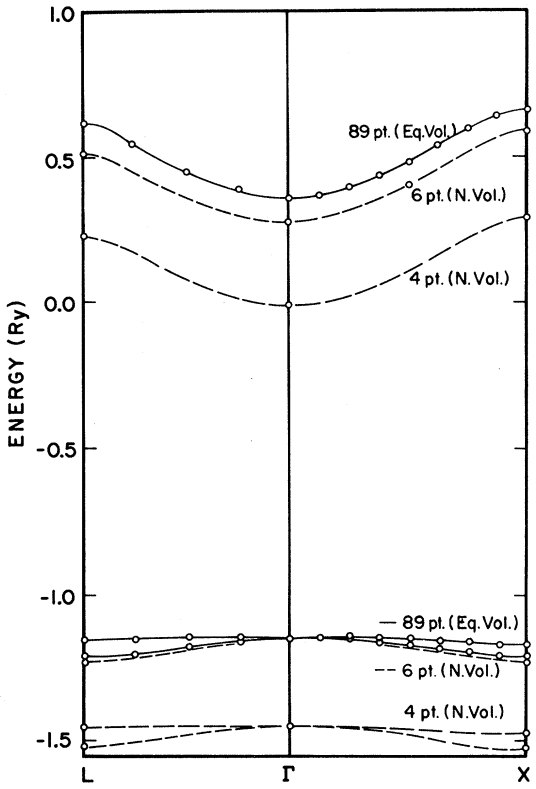

FIG. 4. Self-consistent LiF bands. Comparison of four- and six-point "nearest-volume" grids with the 89-point equal-volume grid.

Explanations for the close agreement between energy differences for the four- and six-point grids are fairly obvious. First, they differ by the addition of only two points, and the two points which were added to obtain the six-point grid lie in the same plane of the Brillouin zone as three of the points in the four-point grid. Thus, both grids attempt to replace a volume integral by a sampling of points in a single plane (ΓXW) and one more point (L) above it. Finally, all six points are symmetry points, which are simply not representative of the vast majority of general points. Unless there is something peculiar about LiF or the equations of Sec. II, one must conclude that previous self-consistent energy-band calculations based on small samplings of the Brillouin zone have errors of the order of eV. This is as much as two orders of magnitude larger than some quoted estimates of errors associated with the small integration grids.

At the risk of making the same mistake, errors associated with the integration grids for this calculation may be estimated. Comparing the 20- and 89-point grids, the bands differ typically by 0.01 Ry. Judging from the trends between the six-, 20-, and 89-point grids, the 89-point grid has an error associated with it which is probably considerably smaller than, but, at most, equal to 0.01 Ry. This is suggested by the computed Fourier coefficients in Table V, the absolute positions of the energy bands, and agreement between the transition energies.

E. Self-Consistent Charge Distribution

A complete self-consistent energy-band calculation offers the opportunity of examining the charge distribution with a model not restricted to the assumptions made in constructing the starting crystal potential. The usual starting point for non-self-consistent potentials has been a linear superposition of atomic or ionic charge densities, the assumption made that there is not much charge rearrangement when the solid is formed. The problem is to decide whether to use atoms or ions and how to determine the effective atomic configuration to be used. An interesting discussion has been given by Slater.[19] The general problem of charge distributions and bonding in molecules and solids has been studied systematically by Pauling[20] and by Phillips and Van Vechten.[21] While LiF is an

TABLE VII. *Approach of energy gap to self-consistency.* The prime grids had equal-volume weights, the unprimed had nearest-volume weights. $\alpha = 1$ exchange parameter was used in each case, but different convergence factors were used for different grids. (Energy units are Ry.)

Iteration	Eg(4)	Eg(6)	Eg(6′)	Eg(20′)	Eg(89′)
0	1.422 40	1.422 40	1.422 40	1.422 40	1.422 40
1	1.426 73	1.424 00	0.840 30	1.488 84	1.450 36
2	1.432 84	1.430 03	0.968 28	1.490 23	1.468 87
3	1.433 98	1.430 94	0.909 66	1.492 07	1.481 22
4	1.434 23	1.431 14	0.905 03	1.492 31	1.489 54
5	1.434 25	1.431 14	0.924 03	1.492 33	1.495 19
6			0.928 92	1.492 24	1.501 70
7			0.926 79		
8			0.927 72		

especially simple case, it is still interesting to examine the self-consistent charge distribution since the paper of Ewing and Seitz[22] suggests covalent or metallic bonding, while Yamashita[23] claims ionic bonding.

Figure 5 shows the change in charge density which occurs when the potential is made self-consistent. While some electrons are moved in near the lithium nucleus, the major rearrangement occurs in the vicinity of the fluorine atom. However, the total charge movement is small. The change in charge near the lithium nucleus was computed by integrating to the first zero shown in Fig. 5 and found to be 0.006 electrons. Integrating further would change this number, depending upon where one chose to define the ionic radius of lithium. Cancellations occur further away from the lithium nucleus, so it is probably safe to say that the maximum charge transferred from the F^- ion to the Li^+ ion is less than 0.01 electrons. In other words, the crystal could be described as fully ionic. An interesting check of this self-consistent result would be to repeat the entire calculation starting from neutral atoms.

V. ANALYSIS OF BAND STRUCTURES

Since the emphasis of this paper has been the self-consistent procedure, exhaustive study of the band structure will not be given now, but will be reserved for a future publication which will include d bands and calculation of the optical properties as well.

There have been several previous investigations of the band structure of LiF. The earliest was done by Ewing and Seitz[22] using the cellular method. Yamashita[23] performed a tight-binding calculation of the coehesive energy and lattice constant, and Kunz *et al.*[24] used a mixed basis method to obtain the band structure. The most recent LiF band calculation was done by Page and Hygh[18] using the APW method. Of the four calculations, the first two gave incomplete band structures, and only the energy bands of Page and Hygh are comparable to the ones obtained here. Kunz *et al.*[24] predict (and attempt to justify with elaborate arguments) that the minimum gap is a direct gap at the L point in the zone. None of the band structures obtained here show this behavior: They are all quite similar to the energy bands of Page and Hygh. Perhaps the results of Kunz *et al.* can be attributed to the details of their potential, but it is more likely just an error in their calculation. Their first-neighbor approximation and spherical approximation to three-center integrals are not adequate for the LCAO part of the LiF Hamiltonian matrix. These errors would be realized in conduction bands as well as valence bands via coupling of bands of the same symmetry. Similar errors probably account for the off-center maximum found by Gout *et al.*[25] in a NaF calculation.

Since the present energy bands agree fairly well with the work of Page and Hygh, numerical comparisons are given here. The SCLCAO energy bands obtained using an $X\alpha$ exchange potential depend upon the choice of α, of course. With the atomic superposition potential, a value of $\alpha = \frac{3}{4}$ gave agreement with the experimental gap. The self-consistent procedure alters the energy gap, so if the exchange potential is to be picked with an appropriate α to obtain agreement with experiment, it must be guessed correctly in advance. Otherwise, the entire calculation must be repeated un-

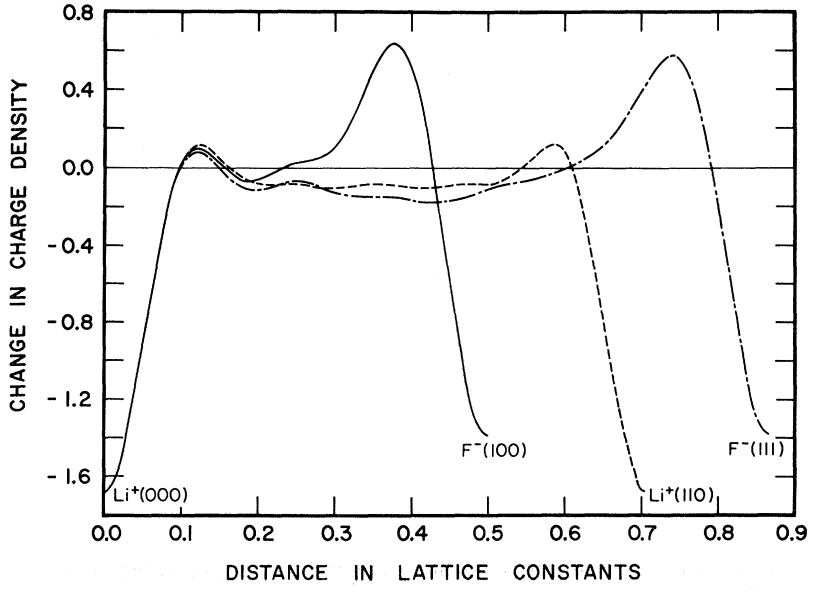

FIG. 5. Self-consistent corrections to LiF crystalline charge density. The unit of charge in this figure is such that if the values shown are divided by A^2, where A is the lattice constant in atomic units (7.5918 for LiF), the negative of the change in electronic density is obtained.

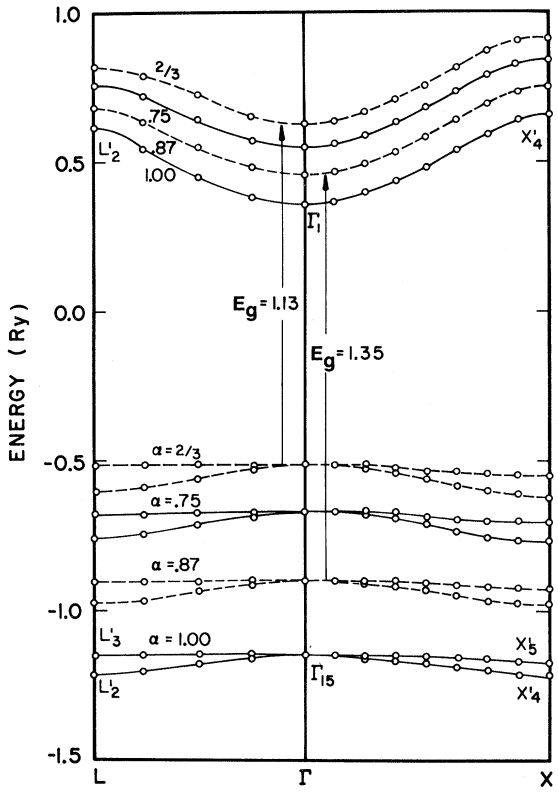

FIG. 6. Self-consistent LiF bands for different $X\alpha$ exchange potentials.

til the desired gap appears self-consistently. Once the generalized overlap matrix S_{ij} has been computed, many self-consistent runs may be done quickly, so several different band structures may be obtained without difficulty. However, other problems do occur, as shown in Fig. 6. With an accurate integration grid the energy gap increases with self-consistency (see Table VII), with the consequence that there is no value of α in the generally accepted range $\frac{2}{3} < \alpha < 1$ which yields a gap of 1.0 Ry: A smaller α would be needed. At this point it was decided to separate the polarization corrections from the band calculation rather than attempt to portray them with the $X\alpha$ local exchange correlation potential.

Polarization corrections to the band energy levels of alkali halides have been computed by Fowler[26] using a static Mott-Littleton-type approach.[27] In this approximation valence bands are raised and conduction bands are lowered by contant amounts: for LiF the amounts computed by Fowler are 1.81 and 2.92 eV, respectively. Thus, Fowler's prescription for fitting the energy gap to experiment is to add 4.73 eV to the observed gap and adjust potential parameters to obtain agreement to the corrected gap. When this was done in the present calculation a value of α was found which was comparable with those found in semiconductors and metals, i.e., $\alpha = 0.87$.

Table VIII compares some of the results of this calculation with the work of Page and Hygh and with various experimental data.[28-31] The following facts must be kept in mind when making comparisons in the table. Since no d orbitals were included in this LCAO calculation, transitions to levels which allow d-mixing may not be accurate, e.g., $X_5' \rightarrow X_1$. The present authors have made no attempt to analyze the optical data, but list the assignments of experimental transitions made by Page and Hygh. A complete calculation of the optical properties of LiF will probably prove some of them wrong. Self-consistent results in the table are headed by the notation SC, while NSC emphasizes the non-self-consistent results.

Considering the different techniques and potentials used, there is rather good agreement between the LCAO and APW results. In the APW calculation nonspherical corrections to the potential were computed by treating all neighbors as point ions. The non-self-consistent transitions with $\alpha = 0.75$ agree closely with the non-self-consistent APW energies. This would not have been the case without nonspherical corrections to the muffin-tin potential used in the APW calculation, since these corrections amounted to 0.8 eV for LiF.[18]

Self-consistent energy bands with a gap equal to the experimental gap plus polarization corrections obtained for $\alpha = 0.87$ are shown in Fig. 6 and column two of Table VIII. Subtracting the polarization correction gave column three of Table VIII (labeled SCP). Once again energies are close to the APW values and in the range of experimental values. The only major change for energy differences occurred for the $X_5' \rightarrow X_1$ transition.

A little reflection upon Table VIII will suggest the following question. Why bother with the labor and expense of a self-consistent calculation if a variation of the non-self-consistent bands via the exchange parameter α will produce nearly the same results?

One answer is that additional experimental information may point out important differences. An example of this is the photoemission edge of LiF, which determines the energy of the top of the valence band relative to the vacuum level. The experiments of Duckett and Metzger[31] indicate a value of 10–12 eV. If polarization corrections for the valence band are made, the value obtained in the self-consistent band calculation falls in this range, but the non-self-consistent results do not. The non-self-consistent APW photoemission edge is far off because of adjustment of $V(0)$ in the muffin-tin potential.

Another reason for obtaining self-consistent en-

TABLE VIII. *Optical transitions*. Comparison of several different calculations with experiment. NSC means non-self-consistent; SC means self-consistent; SCP means SC with polarization corrections. All units are eV.

	NSC $\alpha=0.75$	SC $\alpha=0.87$	SCP $\alpha=0.87$	NSC APW	Experimental[a] A	B	C
$\Gamma_{15}\rightarrow\Gamma_1$	13.7	18.4	13.7	13.6	< 14	13.6	13.5
$L_3'\rightarrow L_2'$	16.6	21.5	16.8	16.4	15.6	14.3	16.0
$X_5'\rightarrow X_4'$	18.7	22.8	18.1	18.5	17.8	17.4	18.0
$L_3'\rightarrow L_1$	20.7	25.0	20.3	20.2	20.8	21.7	21.5
$X_5'\rightarrow X_1$	25.9	28.1	23.4	22.9	23.9	23.0	...
Photoemission	8.8	12.2	10.3	6		10–12[b]	
$V_e(000)$	−5.88	−6.49					
$V_e(111)$	1.60	1.40					
$V_e(200)$	3.95	3.57					

[a]Experimental data as interpreted in Ref. 18. Column A is Ref. 28, B is Ref. 29, and C is Ref. 30.
[b]Reference 31.

ergy levels is to obtain better wave functions. These are needed for the computation of any electronic property, such as the charge density or x-ray form factors. The last three rows of Table VIII show Fourier coefficients of the electronic Coulomb potential. Differences in $V(000)$ account for half the difference in photoemission edges for the calculations in the first two columns. While differences in these Fourier coefficients are not large, they are of the order of 10% or greater. Since the Fourier coefficients may be related to x-ray form factors via Eq. (3), an experimental resolution could be made in favor of one or the other calculations. The self-consistent values most likely would be the better of the two sets, otherwise the "magic" of an atomic superposition must be explained.

Matrix elements for an optical-properties calculation will also depend upon the wave functions, and any such calculation is really not legitimate until the problem has been done self-consistently. This consideration will be discussed in a future publication.

VI. CONCLUSION

A method of performing self-consistent LCAO band-structure calculations has been presented here. The method was found to be quite efficient once data handling problems were resolved. The SCLCAO method works rapidly because of the small secular determinant and the formalism which expresses iterated-Hamiltonian matrix elements in terms of integrals which need to be computed at the first stage of calculation only. In SCLCAO calculations the majority of computer time is spent evaluating integrals if the Brillouin-zone grid is not too large (≤ 89 points). The time required to obtain self-consistency by the present technique represented only about 5% of the total time for LiF.

Accuracy of the SCLCAO energy bands of LiF was estimated by investigating five types of convergence involved in the calculation. By using Gaussian basis functions, large Brillouin-zone samplings (89 points), and convergence factors when computing iterated charge densities, it was possible to obtain an over-all accuracy in energy levels of better than 0.01 Ry for the lowest conduction band, and considerably less than 0.01 Ry for valence bands. These studies suggest that previous self-consistent band-structure calculations reported in the literature contain errors which may be as large as 1 eV. A notable exception to this is found in Ref. 13, which these authors regard as a remarkable paper.

The self-consistent LiF energy bands obtained here were compared with previous work, both experimental and theoretical. By properly adjusting the $X\alpha$ exchange potential it was possible to obtain agreement with theoretical calculations of Page and Hygh as well as with their interpretation of the optical data. While an adjusted non-self-consistent band structure agreed with optical data, only the adjusted self-consistent energy bands agreed with both optical and photoemission data. The importance of using self-consistent energy bands in the calculation of optical properties was stressed.

ACKNOWLEDGMENTS

The authors would like to thank J. Langlinais and N. Brener for many useful discussions.

†Present address: College of Charleston, Charleston, S. C.

*Work supported in part by the U. S. Air Force Office of Scientific Research under Grant No. AFOSR 68-1565.

‡Present address: University of Texas, Arlington, Tex. 76010.

[1]F. Bloch, Z. Physik 52, 555 (1928).

[2]E. E. Lafon and C. C. Lin, Phys. Rev. 152, 579 (1966).

[3]J. M. Tyler and J. L. Fry, Phys. Rev. B 1, 4604 (1970).

[4]F. M. Mueller, Phys. Rev. 153, 659 (1967).

[5]J. C. Slater and G. F. Koster, Phys. Rev. 94, 1498 (1954).

[6]W. A. Harrison, *Solid State Theory* (McGraw-Hill, New York, 1970).
[7]R. C. Chaney, T. K. Tung, C. C. Lin, and E. E. Lafon, J. Chem. Phys. 52, 361 (1970).
[8]J. L. Fry, D. M. Drost, and N. Brener, Bull. Am. Phys. Soc. 16, 405 (1971).
[9]J. Callaway and J. L. Fry, in *Computational Methods of Band Theory*, edited by P. M. Marcus, J. F. Janak, and A. R. Williams (Plenum, New York, 1971), p. 512.
[10]D. J. Stukel and R. N. Euwema, Phys. Rev. B 1, 1635 (1970).
[11]D. J. Stukel, R. N. Euwema, T. C. Collins, F. Herman, and R. L. Kortum, Phys. Rev. 179, 740 (1969).
[12]A. B. Kunz, Phys. Status Solidi 36, 301 (1969).
[13]J. W. D. Connolly, Phys. Rev. 159, 415 (1967).
[14]P. D. DeCicco, Phys. Rev. 153, 931 (1967); W. E. Rudge, Phys. Rev. 181, 1024 (1969).
[15]J. C. Slater, T. M. Wilson, and J. H. Wood, Phys. Rev. 179, 28 (1969).
[16]E. Clementi, *Tables of Atomic Functions* (IBM, San Jose, Calif., 1965).
[17]S. Huzinaga and Y. Sakai, J. Chem. Phys. 50, 1371 (1969).
[18]L. J. Page and E. H. Hygh, Phys. Rev. B 1, 3472 (1970).
[19]J. C. Slater, *Quantum Theory of Molecules and Solids* (McGraw-Hill, New York, 1965), Vol. 2, Chap. 4.
[20]L. Pauling, *The Nature of the Chemical Bond* (Cornell U.P., Ithaca, N. Y., 1960).
[21]J. C. Phillips and J. A. Van Vechten, Phys. Rev. B 2, 2147 (1970); 2, 2160 (1970).
[22]D. H. Ewing and F. Seitz, Phys. Rev. 50, 760 (1936).
[23]J. Yamashita, J. Phys. Soc. Japan 7, 284 (1952).
[24]A. B. Kunz, T. Miyakawa, and S. Oyama, Phys. Status Solidi 34, 581 (1969).
[25]C. Gout, R. Frandon, and J. Sadaca, Phys. Letters 11, 656 (1969).
[26]W. B. Fowler, Phys. Rev. 151, 657 (1966).
[27]N. F. Mott and M. J. Littleton, Trans. Faraday Soc. 34, 485 (1938).
[28]A. Milgram and M. Givens, Phys. Rev. 125, 1506 (1962).
[29]D. M. Roessler and W. C. Walker, J. Phys. Chem. Solids 28, 1507 (1967).
[30]C. Gout and F. Pradal, J. Phys. Chem. Solids 29, 581 (1968).
[31]S. W. Duckett and P. H. Metzger, Phys. Rev. 137, A953 (1965).

PHYSICAL REVIEW B VOLUME 5, NUMBER 2 15 JANUARY 1972

Semiempirical Molecular-Orbital Treatment of the *U* Band in LiF : H^-

Michael R. Hayns*
Quantum Theory Project, Nuclear Sciences Building, University of Florida, Gainesville, Florida 32601
(Received 26 July 1971)

Calculations using the semiempirical self-consistent-field procedure known as complete neglect of differential overlap (CNDO) have been made on a collection of lithium and fluorine atoms in an attempt to generate a model of the *U* center. The system consists of 27 atoms arranged in a fcc lattice. The central fluorine atom is replaced by a hydrogen atom, simulating the *U* center. Calculation of the CNDO eigenvalue spectrum for this "molecular" model shows that the essential features of this defect are represented very well and that the value obtained for the *U*-band excitation energy compares well with empirical and other theoretical data.

I. INTRODUCTION

In a previous study[1] I investigated the feasibility of utilizing a very simple "molecular" semiempirical self-consistent-field (SCF) procedure for the calculation of the electronic structure of ionic crystals. Pilot calculations on LiF using the complete neglect of differential overlap (CNDO) method gave very encouraging results for the bandwidths and band gaps generated from model systems containing up to 18 atoms. Later calculations[2] have extended the size of the model system to 27 atoms, with a consequent increase in the accuracy of the description of the band structure.

The applicability of the CNDO procedure to the calculation of the electronic structure of solids has been supported by the recent work of André *et al.*[3] in their comparative study of extended Hückel, CNDO, and *ab initio* calculations of the band structures of polyene and polyethylene. As these authors point out, the results of semiempirical calculations must be treated with some reserve, however, the relative band characteristics are described reasonably well by the CNDO method when compared to *ab initio* calculations. This is particularly true in the region around the Fermi level, which is where our interest lies in the current calculations. Since *ab initio* calculations on the systems being investigated here are not feasible at the present time, and in the light of previous experience, we feel that the use of the CNDO approximation in this case is justifiable.

In this work we have studied one of the simplest defects in the alkali halides—that of the *U* center.